FY03 LDRD ERD final report for
Project number 01-ERD-072

LAWRENCE
LIVERMORE
NATIONAL
LABORATORY

UCRL-TR-155880

Development of Wet-Etching Tools for Precision Optical Figuring

M. C. Rushford, S. N. Dixit, R. Hyde, J. A. Britten, J. Nissen, M. Aasen, J. Toeppen, C. Hoaglan, C. Nelson, L. Summers and I. Thomas

January 27, 2004

This work was performed under the auspices of the U.S. Department of Energy by University of California, Lawrence Livermore National Laboratory under Contract W-7405-Eng-48.

FY03 LDRD ERD final report for Project number 01-ERD-072

Development of Wet-Etching Tools for Precision Optical Figuring

NIF Directorate

M. C. Rushford, S. N. Dixit, R. Hyde, J. A. Britten, J. Nissen, M. Aasen, J. Toeppen, C. Hoaglan, C. Nelson, L. Summers and I. Thomas

Contact Info: Mike Rushford
Tel: 4-6349 Fax: 4-6333
E-mail: rushford1@llnl.gov
Mail code: L-474

Executive Summary

This FY03 final report on Wet Etch Figuring involves a 2D thermal tool. Its purpose is to flatten (0.3 to 1 mm thickness) sheets of glass faster thus cheaper than conventional sub aperture tools.

An array of resistors on a circuit board was used to heat acid over the glass Optical Path Difference (OPD) thick spots and at times this heating extended over the most of the glass aperture. Where the acid is heated on the glass it dissolves faster. A self-referencing interferometer measured the glass thickness, its design taking advantage of the parallel nature and thinness of these glass sheets. This measurement is used in close loop control of the heating patterns of the circuit board thus glass and acid. Only the glass and acid were to be moved to make the tool logistically simple to use in mass production.

A set of 4-circuit board, covering 80x80-cm aperture was ordered, but only one 40x40-cm board was put together and tested for this report.

The interferometer measurement of glass OPD was slower than needed on some glass profiles. Sometimes the interference fringes were too fine to resolve which would alias the sign of the glass thickness profile. This also caused the phase unwrapping code (FLYNN) to struggle thus run slowly at times taking hours, for a 10 inch square area. We did extensive work to improve the speed of this code. We tried many different phase unwrapping codes. Eventually running (FLYNN) on a farm of networked computers. Most of the work reported here is therefore limited to a 10-inch square aperture.

Researched into fabricating a better interferometer lens from Plexiglas so to have less of the scattered light issues of Fresnel lens groves near field scattering patterns, this set the Nyquest limit.

There was also a problem with the initial concept of wetting the 1737 glass on its bottom side with acid. The wetted 1737 glass developed an Achromatic AR coating, spoiling the reflection needed to see glass thickness interference fringes. In response to this dilemma, the acid wetting was moved to the top of the glass and the thermal diffusion layer under the glass replaced with rubber. The bottom side of the glass was then protected from etching with a vacuum grease layer on the glass, though many other ways were tried and need to be further developed.

We switched our mission away from flattening the OPD of 1737 glass, as the Eyeglass project no longer wanted glass. We turned our attention to the NIF Borofloat Debris shields.

FY03 LDRD ERD final report for
Project number 01-ERD-072

The NIF Borofloat glass comes with a 30-micron wedge over 30 cm lengths making finely spaced Fizeau fringes and at times aliases in this self-referencing interferometer design. The solution we settled on was to measure this glass when its topside was dry, as this maximized the visibility of the interference fringes, making a better measurement of the glass wedge. We then showed this wedge could be removed in 1-2 hour of process time. Much faster times were possible but only if Wet Etch Figuring was run in a dead reckoning manner, for 90% of the required work.

The interferometer measurement and analysis were to slow to deal with the speed that was possible from this parallel thermally driven figuring tool. On a thirty minute interval the acid would be removed from the glass and the new glass OPD measured and a heating pattern applied until the glass OPD profile was within 1-2 micron of a uniform. Then we would slow the acid dissolution rate and allow the interferometer to close the loop, as we now had removed all the finely spaced interference fringes, which now allowed the unwrapping code to turn around every 30-60 seconds.

For a NIF related demonstration we calculated how this flattened OPD glass would perform if propagated to NIF focal spot formed by a phase plate creating a 1 mm spot profile. The energy in a bucket with and without this measured debris shield glass was measured. A targeted difference goal of 5% over all radii from spot center established for 3W light. We achieved 7% difference over a 10-inch Borofloat glass size, so we say 5x more improvement is needed from this work to satisfy NIF @ 3W.

This experience indicates it is possible to OPD flatten one piece of Borofloat glass per day with one machine. However, further experience and redesign of logistics would improve this technology.

FY03 LDRD ERD final report for Project number 01-ERD-072

Table of Contents

FY03 LDRD ERD final report for Project number 01-ERD-072

Introduction

Optics have been in use for a long time in a variety of applications ranging from camera lenses to space telescopes to high power lasers. The present approaches for figuring large aperture optics consist of grind and polish, small tool figuring, magneto rheological finishing and plasma etching. These techniques are expensive and involve large capital investment. For applications involving high power lasers (ICF, Petawatt) and in high resolution imaging, a high degree of optical finish is desired. Typically, transmission wave front is required to be of the order of $\lambda/10$ or better. Large apertures are also required in high power lasers to minimize the laser damage and in space telescope applications to enhance the signal to noise ratio (achieved due to increased light collection). The combination of high optical quality and large apertures drives up the fabrication costs for such optics. There is a need for developing low cost finishing techniques for high quality optics at large apertures.

FY03 LDRD ERD final report for
Project number 01-ERD-072

FY01 ER effort:
Marangoni confined wet-etch process development

In FY01 we received $ 189 K LDRD ER funding for the development of wet-etch based surface figuring processes for optical finishing (ref 1,2,3). Material removal on optical surfaces can be accomplished by etching or dissolution methods (e.g. silicate glasses are soluble in hydrofluoric acid solutions). Wet etching using buffered HF solution has been employed by us for fabricating phase plates for Nova laser applications. The problem in applying this method for surface figuring had been largely how to confine the wetted zone of etchant solution to a specific stable geometry. This was solved by taking advantage of the Marangoni effect where a surface-tension gradient (caused by the dissolution of a small amount of alcohol vapor) confines the wetting region. We built a point etch tool based on this effect and also a 6" wide 1-d line etcher tool. Figure 1 shows the view near the etch application region for the point etch tool. Both these tools have been successfully used surface figuring of thin glass sheets. In figure 2 we show examples of a surface flattening achieved with a 1-d etcher and also a phase plate for compensating the phase of the laser beam in a high-power laser. This research has been very well received by the community and has generated interest from the industrial community.

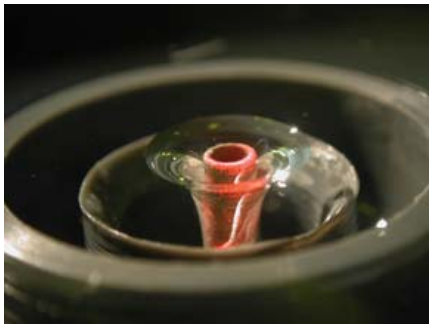

Figure 1. Picture of a Marangoni confined wet etching region.

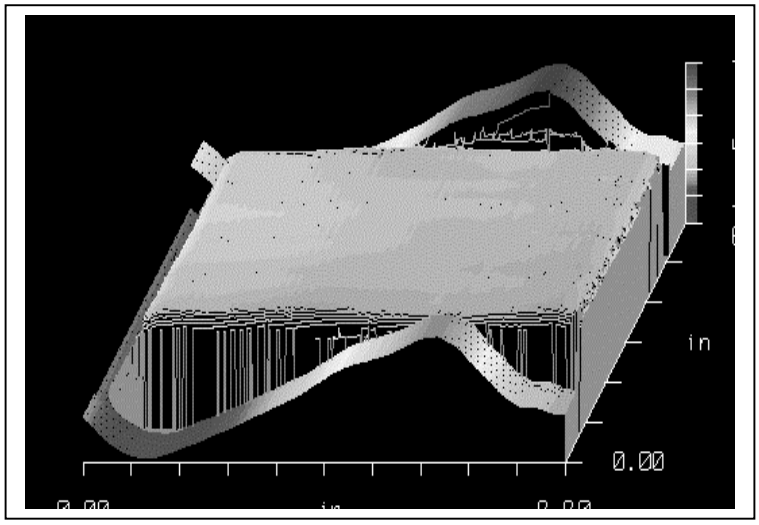

Figure 2a. Transmitted wavefront of 150 x 200-mm section of Corning 0211 380 micron-thick glass plate flattened using linear etching tool. Approximately 9 waves of distortion in transmitted wavefront has been removed, leaving ~ 1/2 wave of residual 2-dimensional error across the part.

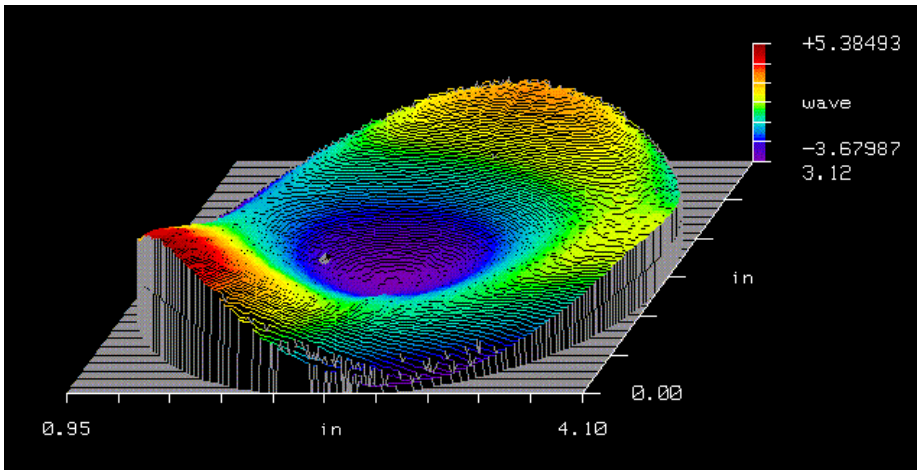

Figure 2b. Interferogram of an 80-mm diameter static wave front corrector for a high power laser, fabricated with automated fountainhead wet-etch figuring tool. Glass thickness Peak to Valley is 12 microns.

FY03 LDRD ERD final report for Project number 01-ERD-072

FY02 ER effort: Development of 2-d parallel etching tools

In spite of the success of the wet etch figuring tools demonstrated in figure 2, these tools are inherently slow when figuring large areas. Fully 2-dimensional surface figuring offers tremendous savings in the etching time for large aperture surfaces. The following table compares the etching times for removing a 10-µm thick layer from a 400 x 400-mm wide region.

Tool	**Etch rate (nm/min)**	**Effective tool foot print**	**Etch time for 10 µm thick material removal over a 400 x 400 mm area**
Fountain head	50	10 mm x 10 mm	**320,000 min** (222.2 days)
Line etcher (not capable of arbitrary 2-d surface figuring)	50	10 mm x 400 mm	**8000 min** (5.6 days)
2-d etcher	50	400 x 400 mm	**200 min** (3.3 hours)

The enormous savings in the etch time come from the simultaneous etching of the entire 2-d surface as opposed to a tool footprint size etching in the case of the fountainhead tool. Even a 10x rate enhancements to the point and 1-d etch process do not achieve the fast etch times implied by the simultaneity of the 2-d etch. Given the tremendous advantages offered by a 2-d differential figuring tool, we believe, it is important to focus on the development of a 2-d differential etching process and demonstrate its utility for surface figuring.

The effort in FY02 involved the development of the 2-d wet-etch figuring process for surface figuring. Just as was done in the point- and the 1-d etcher case, continuous monitoring of the wave front and feedback to the etchant delivery are both necessary for a controlled etching process. Rapid, in situ gathering of the surface wave front data is needed in order to make the etch process closed-loop. To realize this, we built a large aperture Fizeau interferometer, ref 5-11, that is capable of measuring the wave front of up to 1 m size thin sheets. A schematic of this apparatus is shown in figure 3. Here a large aperture, inexpensive Fresnel lens collimates light from a laser. The light source is located slightly away from the lens focus in order to introduce a slight tilt to the collimated light. The reflections from the two surfaces of the glass under interrogation gives rise to the Fizeau fringes in the reflected light. To convert the fringe map to a wave front map requires capturing the fringe maps either at different tilts or at different wavelengths. We chose the latter approach, for glass thickness between 300 and 1.1 mm thickness, as this does not require any movement of tilt mirrors etc. and reliable frequency scanning lasers are commercially available. An example of the four fringe pattern frames and the resulting smooth wave front are shown in figure 4.

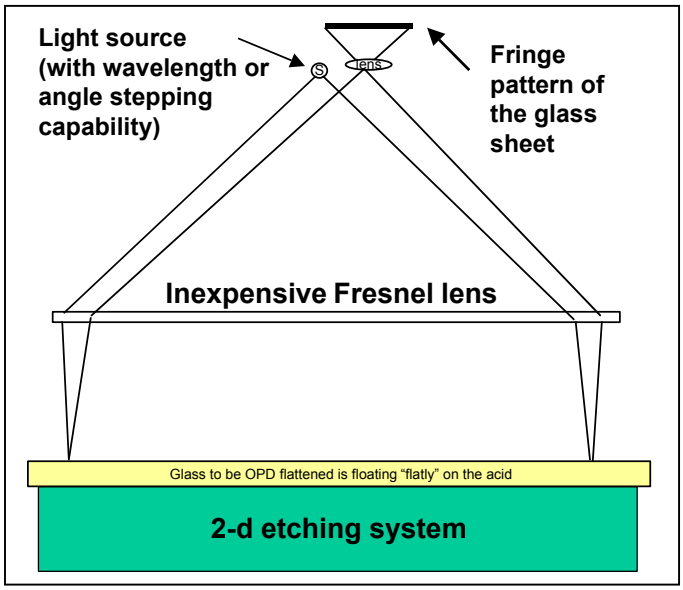

Figure 3. A schematic of the Fresnel lens based Fizeau interferometer for measuring the wave front of large thin glass sheets.

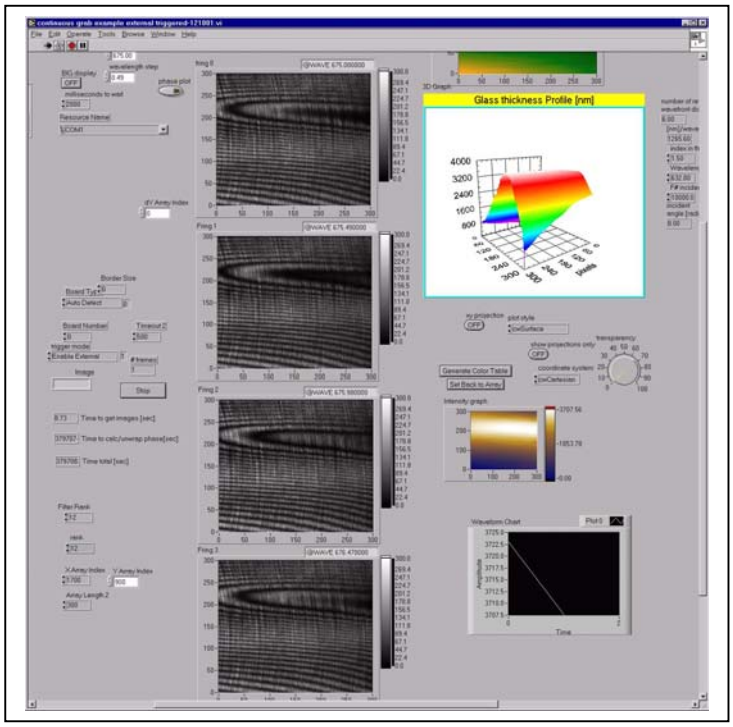

Figure 4. Fizeau fringe pattern for the four wavelengths used in the interferometer. The unwrapped optical wave front map is shown in the picture in the upper right.

In parallel to the interferometer development, we explored a variety of parallel etching approaches.

Heating methods (ref 4) that we tried included;
Hot air onto the glass while in contact with acid.
Electrical resistors and wires in thermal diffuse contact with the acid or glass.
High power IR light source contact printing and projection of gray-scale masks.
3-micron laser light through the glass absorbed at the acid glass interface.
Microwave arrays would also be an interesting investigation.

Non thermal methods were also tried, generate the HF etchant in situ using an electrolytic process, high speed acid printing.
Some of these techniques have been shown to be of little promise. Others merit further investigation.

In developing a parallel etch process, the properties that can be taken advantage of are the variation of the etch rate with temperature and concentration. Typically, the etch rate doubles with a 10 degree increase in temperature. If one could locally heat the etchant solution, then one could differentially control the local etch rate. A 2-d surface can then be figured in a short time scale.

A second approach we investigated was to differentially apply the etchant solution simultaneously over the 2-d surface. The etchant solution was applied using a ink-jet head that rapidly scanned over the part and deposited the acid over thicker regions. Here we were able to remove approximately 1 μm worth of material from the glass and also observed some flattening. The difficulties with this approach were the need to maintain the required concentration gradients and to be able to stop etching at a predetermined point. At present, we have tabled this approach.

We also examined an electrolytic approach for differential etching where in the etch component (F-ions) are generated in situ near a positive electrode and etch the glass held in proximity to it. The advantage of this approach is that there is no background etch. The differential nature of etching can be achieved by individually controlling an array of electrodes. This approach looked very promising. We demonstrated differential etch rates of 100 nm/min or higher with very modest (~10V) voltages. The drawbacks observed were the generation of particulate precipitates and also the erosion of the electrodes.

FY03 LDRD ERD final report for Project number 01-ERD-072

FY03 Current results

Design, construction, debugging and software developments of the Circuit board Wet Etch Figuring heater.

A set of 4 each ~40 cm square circuit boards systems were ordered but only one was populated with its chips and powered for this first test.

A thermal image circuit board heater was designed (Ref 12,13,14) for flattening Shot glass type 1737. Each pixel consists of a resistor and a Logic gate on a 64 x 64 array with 7-mm pitch (42x42 cm). The (64x64 image array) of logic gates were sequentially scanned at 10 HZ and each gate turned on or off depending on each of 1024 different images, stored in onboard memory. This commercially available PCB technology and components provided 200 W total power over NIF size parts. The power output, of the first prototype was 5 times below design request due to parts availability. The pixel heating had 1024 levels of temperature which could be digitally assigned through; parallel port interface, taking 30 seconds to load. During the memory load, the power to the resistor array was turned off. Adding jumpers to this design would allow fewer gray levels, thus shortening the time to update a new thermal image. In retrospect, with dual ported memory, a pulse-width modulated heating control would have avoided the transient response due to shutting down the thermal image power during the memory write cycle. It cost ~ 5 K to build one board, ~ 17K to debug and write software drivers. The software drivers were further reworked for a 20 x speedup.

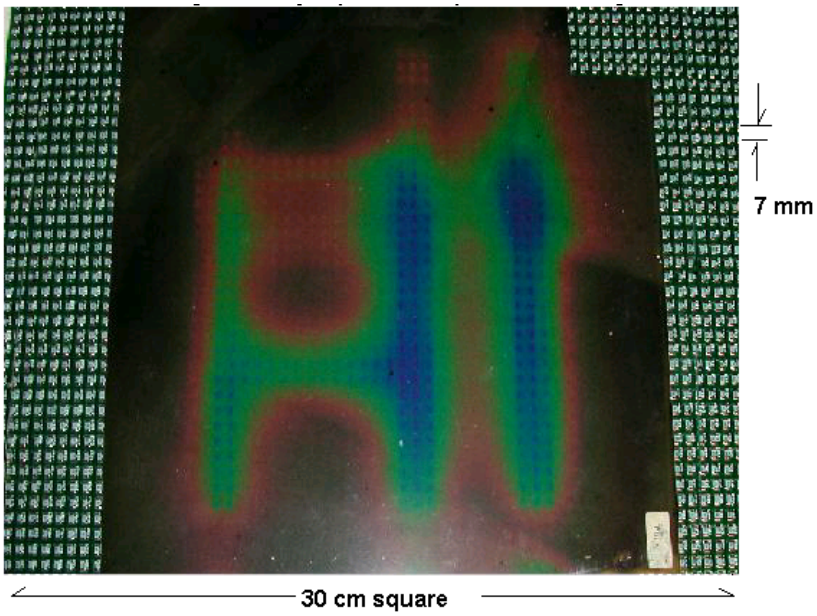

Figure 5. Test of the 2-d addressable resistor array. Showing 5 C temp range, from 25-30 C. There is cross talk (pixels a little hot which should not be hot at all) as seen above the letters, during this test.

Writing a thermal image Figure 5 to the resistor array was visualized using "CHOLESTERIC liquid crystal paper" laid over the full resistor array. This enabled viewing the thermal image for hot spots, intentional or not. Shorts and other anomalies, pictured in Figure 6 and cross talk, pictured in figure 7 were seen and corrected. Further repairs were needed during initially mounting the board on it heat sink. The shorts were induced by static discharge, which developed when lifting the circuit board from the thermal grease on the heat sink. Dismounting the circuit board from its thermal contact of grease was required to replace several chips. The original design was H-Grease, but due to its high cost vacuum grease was substituted for thermal contacting to the circuit board. The plastic insulator

was heat sunk to the water-cooled aluminum plate using industrial hydrocarbon grease.

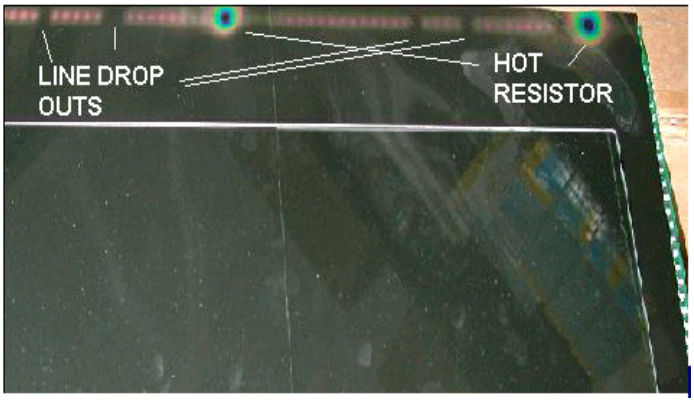

Figure 6A. Initial testing the 2D-resistor array showed shorts on a line near the circuit board edge and other anomalies. The circuit board was re worked at the 321 circuit board shop.

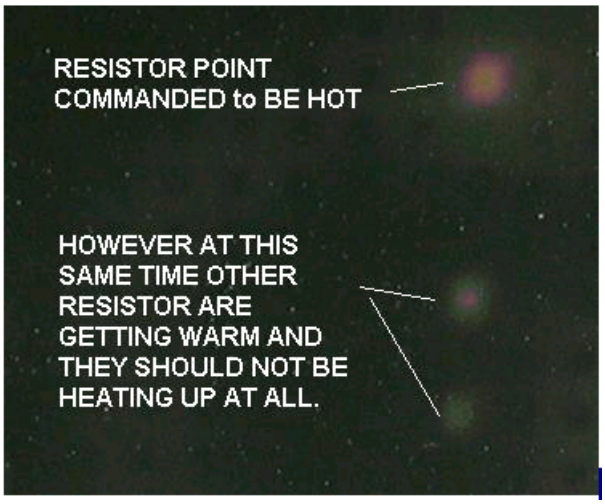

Figure 6B. There were ghost resistor partially heating at the same time. The address position of the ghostly heated resistor is always correlated to the X-axis line driver chip, which is addressing the one point to be heated. The ghost column moves one to the right as the row position of the heated resistor is moved down. The issue was resolved by adding bypass capacitors.

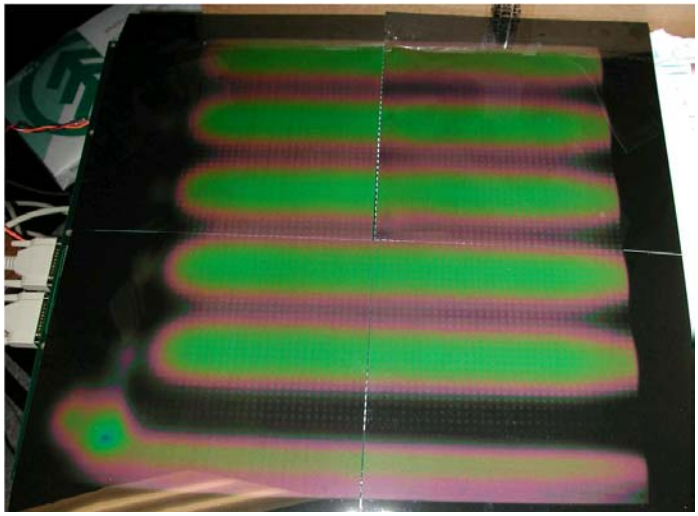

Figure 7. The circuit board is shown test heating (where green) 5 sinusoidal thermal patterns. This illustrated the wavelength of the thermal pattern needed to make corrections on 1737 glass. Bottom left hot spot is a failure point we chose to ignore for now.

Writing the 1024 images to memory took 30 seconds. Writing fewer images would take less time. This change was not implemented due to the potential damage it would do to the board, but should be implemented on the next generation board. In fig 7 the board still has some shorts along the bottom and left edges but in the middle it works well enough to continue with assembly and testing the rest of the concept to be studied.

Thermal Modeling;

A 1D thermal diffusion calculation for the required heating pattern, fig 7, needed to correct Shot glass type 1737 thickness ripples guided the circuit board design. It was estimated that a 6 mm thickness of plastic insulation between the heat sink and circuit board, along with ~6 mm thickness of heated acid above the heaters, with the glass on top, would be a best first try. A 2D thermal diffusion calculation illustrated advantages for moving the glass around to overcome printing in the fixed pattern of heaters. Moving the glass when it was floating on top the heated acid would be used to overcome the fixed pattern print through likely to occur using this array of resistors.

Design and Construction of the heat sink, acid confinement, glass handling and mounting.

Ultem plastic was chosen as a thermal resistance and acid containment construction material as it came with a complete technical description and was solvent weld-able. The construction of the Ultem acid tray via solvent welding did not work due to internal stress induced during water jet cutting this material. We tried to straighten it to a flat shape between two 80-cm SiO2 plates at 91 C

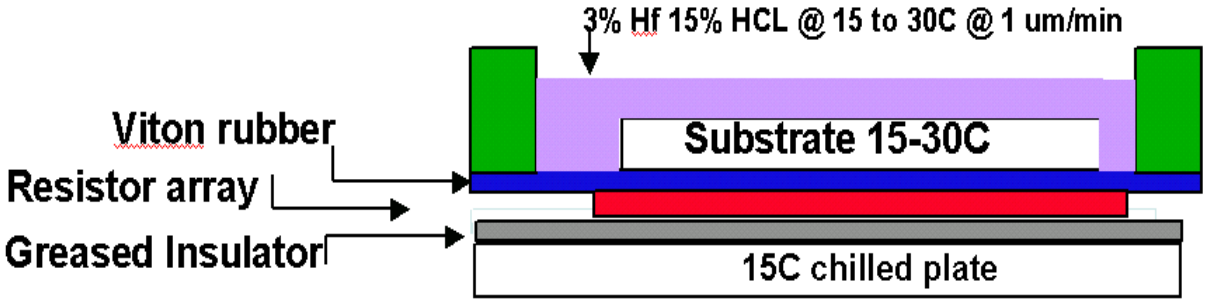

Figure 8. Schematic cross section of thermal 2D Wet Etch Figuring tool.

for three hours, but it never looked promising. We then constructed another acid tray bottom from Mylar and the sides from Plexiglas. Contact cement (region C in Fig 9) made an acid tight seal between the Plexiglas rim and Mylar base (region B in Fig 9). The Plexiglas container was solvent welded together.

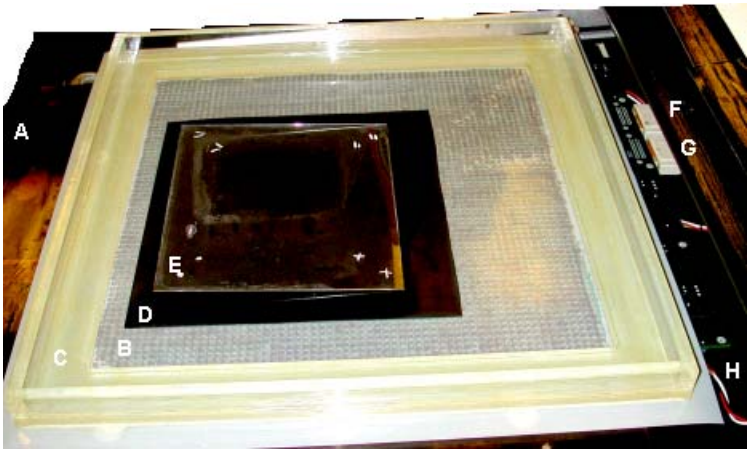

Figure 9 Prototype 2D thermal Wet Etching Tool acid containment

The last trial construction that satisfied many of the logistic is shown schematically in Fig 8, the real system in Fig 9. A water-cooled aluminum chill plate is vacuum greased on top to make thermal contacted to 6-mm thick Ultem plastic insulator. This plastic was counter sunk screwed down to the chill plate. Vacuum greases on top the plastic provided heat sinking to the bottom side transistors of the circuit board. The circuit board was #00 screwed to the Ultem plastic, through holes in the circuit board between the conductive traces. Vacuum grease was spread on to the topside of the circuit board to a level planar over the surface mounted resistors. Onto this grease, the acid container was laid in thermal contact. The bottom of this container was a flexible material. Our first attempt was five mills of Ultem then 30 mil of Mylar and finally 4 mm of Viton. Ultem or Mylar eventually adsorbed water and would have to be dried with heat guns before it would lay flat after being wetted for a few days, this is main reason why we switched to Viton. The thickness of the Viton was to be explored as the means to remove the fixed pattern print through of the resistor heating array, though never varied from its 4 mm thickness for all this work. To make this bottom layer (region B fig 9) lay flat a 4-inch diameter steel roller pin was rolled around on top this rubbery layer (region D fig 9), to redistribute the grease underneath (region B fig 9). The glass substrate

backside was protected from the acid etching by smearing vacuum grease over its bottom side. Other ways to protect the back of the glass were tried; water itself, masking tape, photo resist, vacuum pump oil, various paints, each had their issues. The vacuum grease was the best in providing a large index of refraction miss match to glass as this increased the interferometer fringe contrast. Suspicion (not verified) is the grease-entrapped lots of air at the glass interface, leading to the large index mismatch to glass. Grease was also more easily applied and removed compared to the other approaches. Water was then put onto the rubbery (region D fig 9) acid bottom, just enough to wet the rubber where the glass was to lay on it. The greased side of the glass was laid onto this water which put the glass in a floating position helping to ensure its flatness so it could reflect light into the interferometer over its entire aperture. Excess water was sucked up and removed from around the glass so it would not create an excessive dilution of the acid.

A measurement of the glass OPD was then made while the topside of the glass was dry and the circuit board turned off. This gave us time to overcome and research issues about the measurement and the commands that would be sent to heat the circuit board. Once we convinced ourselves the measurement was correct, we would command the circuit board to begin heating. The heating was restricted in many different experimental trials as we sought a best strategy in reaching our glass-flattening goal in the shortest possible time. The preferred method was to begin heating the glass and wait 15 minutes for it to overheat to 50-60 C. This allowed time for thermal cross talk, which helped prevent printing of the fixed pattern of the heating resistors. The stored latent heat within the tool helped to maintain the etching speed after the acid was poured onto the heated glass.

The acid was poured from a beaker onto the glass substrate and later vacuum pump removed. A better solution, for the next generation hardware, is to tip the tray on end and spray the tray with water to stop the acid etching.

With the glass now wet with acid, we could still see the Fizeau interference fringes and these contour fringes moved uphill disappearing as the glass began to flatten. The fast rate at which the fringes now moved prevented real time control. We could not guarantee the timing needed to take the four each interference fringe images needing to be at 90 degree fringe shifts, required for phase unwrapping.

At first, large glass removal rates of 1-2 microns per minute occurred at the high spots, which were heated to 30-60 C. At the cold spots at 10-15 C, 5-6 time less was removed.

There was fog-steam at times above the heated acid and this deposited fluorite, visible as a white layer on a glass, 10 inches above this heated acid. Therefore, we did not try higher temperature or acid that is more concentrated.

Example of using this tool;

With the apparatus shown in Fig 9 we flattened a 0.7-mm thick 25x25-cm sheet of Corning 1737 glass, obtaining the results shown in Figure 10. On the right, of each of these three A, B, C different time snap shots, is the interference fringe measurement of the glass thickness. This was simultaneously converted to a gray scale image upper left and its overlaid with the interference fringes used to inspect for aliasing induced glass thickness sign reversal. The gray scale part of this image was then scaled to fit the array of resistors under the glass. The full 64x64-array of heater positions is shown in the lower left with the sub array-heating image written into the 1024 image layers of the circuit board memory. The glass being worked here is 10 inch square indicated by the white square frame. Around this frame, heating is extrapolated beyond the glass edges to improve the edge of the glass results. The gray-scale heating threshold was explored and typically limited to work the top 100 to 60% of the glass thickness profile. Only thermal diffusion heating could then reach the thinner parts of the glass thickness profile. Additional, gamma and contrast gray scaling was applied experimentally as we explored for a best result. In this test fig 10 half of the 5 microns of 1737 glass ripple was removed in 30 minutes and appeared to come to a stop even though heating was maintained. The acid was then vacuum pump removed and fresh acid poured on to resume the rate of glass removal at the 1-hour time (Fig 10 B). The glass came to a slowed etching after 30 minutes (Fig 10 C). The glass now showed some roughing imposed from the manual cleaning and acid replenishment procedure. This result prompted us to seek addition funds toward this LDRD effort so to reengineer the acid delivery and removal in an automated way every time the rate of removal appeared to slow. The effort was not funded so we turned our attention to the remaining part of the year to improvements of the interferometer code speed and investigated other types of sheet glass.

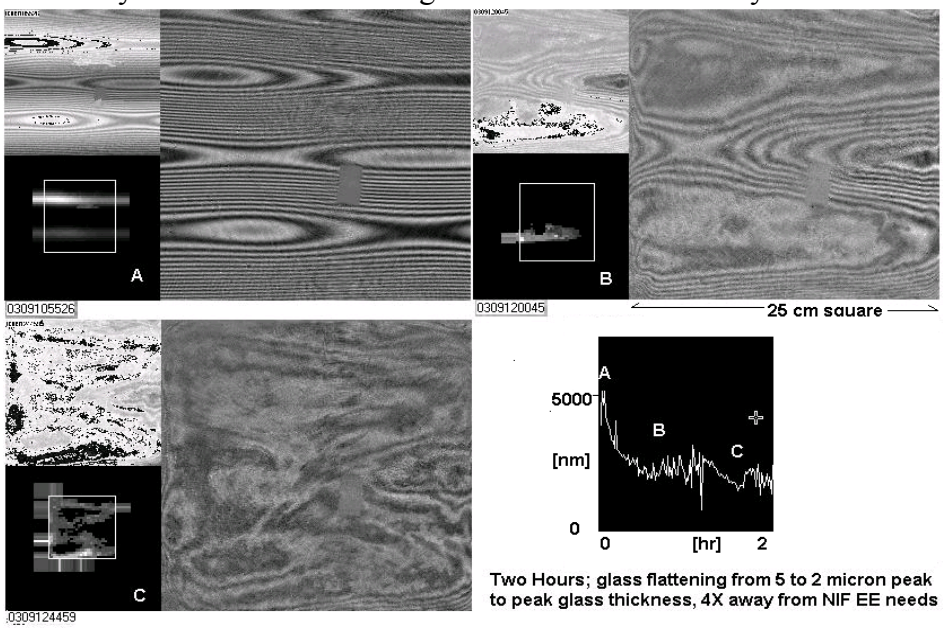

Figure 10. Three different times labeled A, B and C during a 2 hour run show the 1737 glass flattening progress.

Broad band AR coating of 1737 glass;

We got sidetracked in our first 40x40 cm 1737 glass aperture trial at using this technology. The 1737 glass was floated on the acid as a boat with sides made from masking tape and this protected from acid with contact cement coating. Docking the boat to a movable platform allowed moving the glass around to help overcome the fix patterns, which would occur from the heating pattern. The 1737 glass floating on acid developed a broad band AR coating, which reduced the reflectivity of the acid wetted glass bottom side causing the interferometer to fail in closed loop figuring, due to bad glass

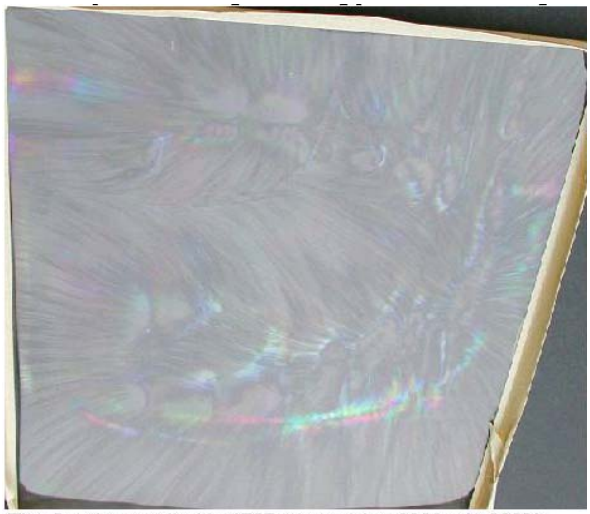

The Coating applied to 1737 when using 2000 ml of 20% HCL brew on the 2D circuit board tool. The streaks in the coating indicate a boyancy (maybe) driven flow. Warmed acid flow up from the heat source to the glass bottom and moves laterly to the unheated places.

Figure 11 AR coating applied to 1737

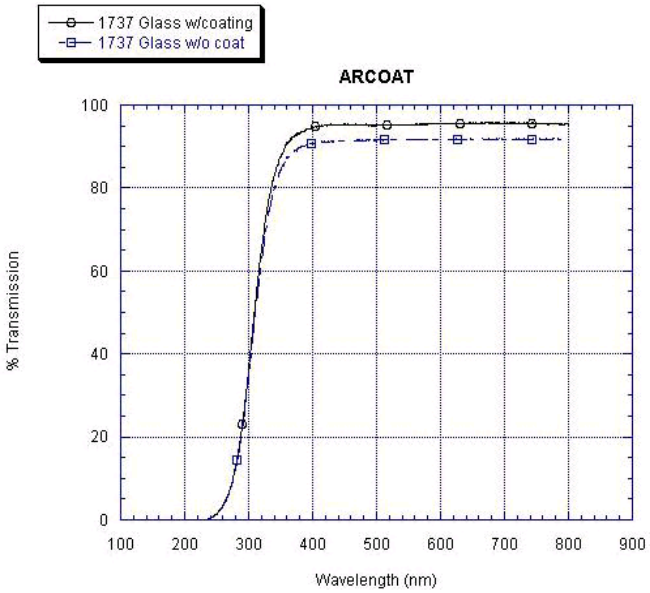

Figure 12 Achromatic AR coating

thickness measurements. Figure 11 shows the coating uniformity seen in reflection over a 30 cm^2 region. Various things were tried to eliminate these coating phenomena. The 1% Hf 15% Hcl Brew was diluted 10x to 0.1% Hf and heated to make the coating. Beaker tests with this dilute acid without heating did not reproduce these coatings. The coating was made on three different glass sheets. It was robust to mechanical abrasion of usual cleaning process and could be removed with HF etchant. The reflectivity is uniformly reduced by 3% across the spectrum Fig 12. This coating may have a graded shape, mass or index profile (ref 5,6,7) with coating depth resulting in this Achromatic AR coating. This indicated some feature of the process we did not understand yet was at fault. It was this coating problem, which suggested putting the glass at the bottom of the acid rather than floating on top the acid.

Glass moved from floating on acid to cover with acid.

To confirm our understanding of this tool and to overcome the AR coating problem seen on 1737 we tried to eliminate the 6-mm of heated acid diffusing layer from between the heating resistors and the glass bottom. This effort removed the acid from the bottom of the glass, so to avoid

Figure 13 Beginning on left to stop on right showing 6 microns of 1737 ripple removed. Here the glass was water contacted to the Mylar. This thermal layer was now so short that the resistor pattern printed into the glass as seen in the interference fringes on the right image.

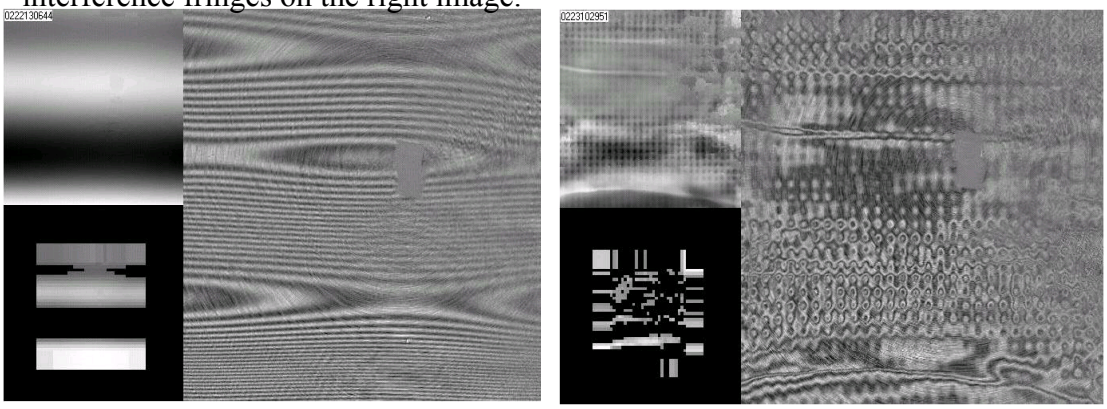

the AR coating problem and buoyancy issues. The upper left Figure 13 is the glass thickness contour. Lower left the heating applied to the 64x64 resistors on the circuit board. On the right the interference Fizeau fringes seen in reflection with the glass wet on both its surfaces, water below acid on top. The fringe contrast remained high since no AR coating occurred on the bottom of the 1737 glass. The glass is lying on the acid container bottom made of Mylar. This allowed printing into the glass a fixed pattern at the resistor spacing (right side interferogram fig 13). Heating occurs below the Mylar and a thin layer of water is between the Mylar (region B Fig 9) and glass bottom. The glass framed with masking tape was now filled with 6-mm depth of acid. Now the glass is heated more directly. The buoyancy now carried the heated acid up away from the glass. The AR coating problem did not occur in this configuration so we continued to develop this concept. In this test 6 micron of peak to peak glass flattening occurred, although roughened by the lack of thermal diffusion between the resistors and glass bottom. Since the 1737 did not get its AR coating recently (glass submerged) we continued using this new setup with 1737 still used to tune up the process.

We started using the NIF focal spot encircled energy calculation (Fig 17) as a metric of glass flattening performance. This test result (Fig 13) was not NIF acceptable, due largely to the resistor pattern printing into the glass. We got rid of this fixed pattern noise using 4-mm thickness of Viton rubber between the glass and resistors (Fig 10 results). We then got 5 pieces of NIF Borofloat to be OPD flattened. Fig 14 is Borofloat made to be parallel and is one of the last results of this work.

Interferometer development and the phase unwrapping evolution:

The first LLNL phase unwrapping codes, written in LabView was fast but had troubles at times when faced with various discontinuities in the fringes. We explored other phase unwrapping code to find one more robust to noise than ours was. An existing library Ref 8 of phase unwrapping code written in C was modified to work with LabView. We tried five algorithms from this library

(Flynn, Goldstein, PCG, Quality and FFT). We found that with ideal phase maps all algorithms worked very well, but when confronted with more complex fringe patterns and noisy images each algorithm had problems and limitations. The FFT based algorithms were fast, but became confused by high fringe density. This method required a 2^n-1 square array. The Flynn algorithm had no array size restrictions and gave good results. Its main problem is execution speed. It would sometimes take half an hour for our computer to run the FLYNN codes, which was unacceptable. The Flynn code also had problems in the corners of the data array, which we had to experience experimentally and eliminate. There was missing data in some of the columns from the camera image that we had to discover and eliminate from the phase unwrapping attempts.

One solution to increase the speed of the phase unwrapping algorithm was to split the data into small parts and use several computers to do the calculation. This distributed computing method was able to unwrap the phase about ten times faster than a single computer. The main problem with this method was that the results from each computer had to be recombined. Each subset of the result had to line up with its neighbors. Most of the time there would be some sections that would not line up correctly. An algorithm was developed to first stitch together each section individual section with its adjacent neighbors and then measure the discontinuity around the four sides. This generated a quality map, which would guide the rest of the stitching process.

We developed another algorithm and interferometer to test a faster possible measurement of the glass. In this case, an optical encoder was used to measure the fringes from a point interferometer. The optical encoder does the phase unwrapping in electronic firmware so is much faster than the LLNL video-based hardware and software. The problem with point wise interferometer is loosing the fringes due to obscurations of the laser light on the thin glass. The loss of fringes causes the encoder to skip counts and count wildly large displacements. These obscurations occur randomly over the entire surface. Returning to the start of a scan would show the total encoding error.

To overcome this problem, the glass is first measured over a dense serpentine column path up one column and down the next and then again over a sparse orthogonal left-right and right-left row paths.

The column path data is adjusted to match these rows values. To ensure that this row data set did not contain discontinuities, each row pair was scanned forward and backward making a closed thin rectangular path. If the position measured at the end of the CW and CCW, paths did not match, then there was a problem and that row data pair was ignored.

This software method was tested on the LLNL video-based hardware and improved the point wise WEF tools.

We did not have the space logistics to try the new optical encoder approach on the 2D thermal figuring tool. Many other interferometer modifications and codes remain to be explored.

Alignment of the interferometer pixels to the resistor pixels;

The alignment between the camera and the circuit board was a problem. We visualized the place for each heated resistor by placing cholesteric liquid crystal paper on the Viton rubber (region D fig 9). We created a matrix, visually assisted, of heated resistor positions seen in the CCD image of the interferometer camera and used this pixel coordinate, as pointer, into the array of OPD data for the glass sheets. Larger arrays showed image distorted by interferometer pincushion distortion. Without correction for this, the circuit board would heat up the wrong region of the glass and create large

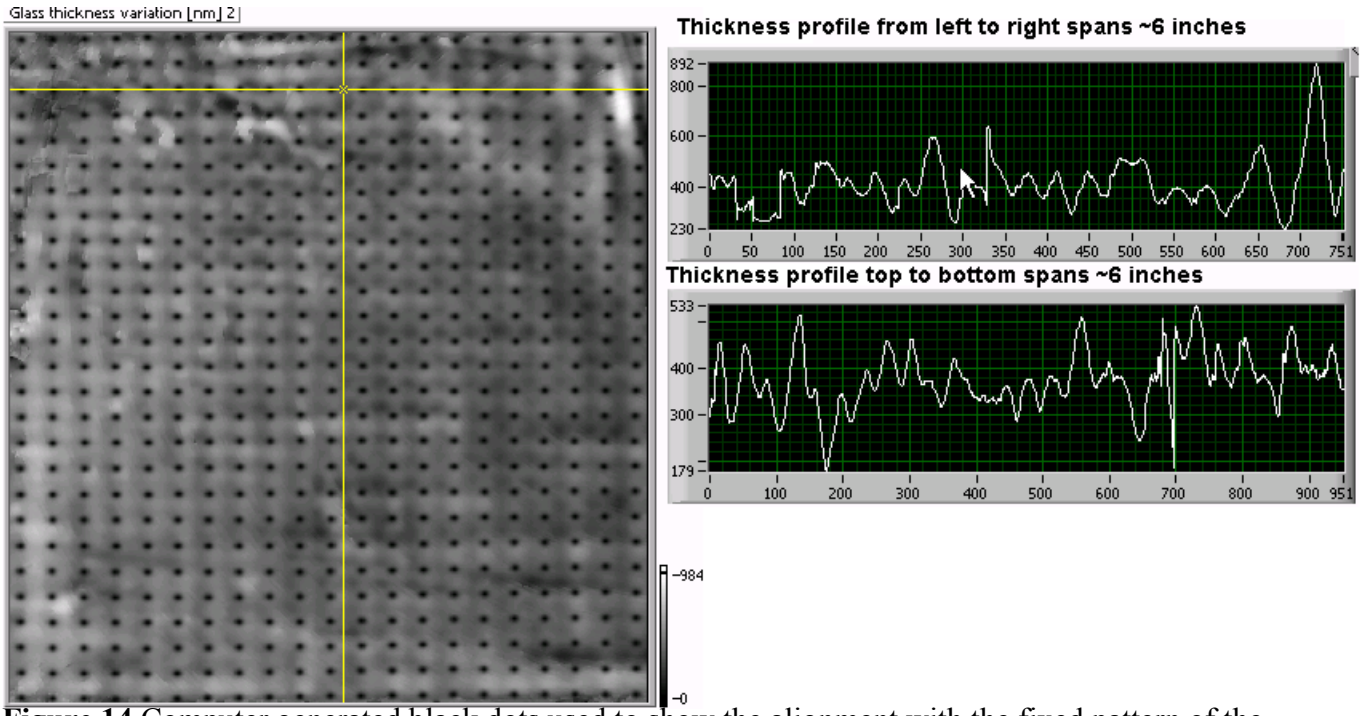

Figure 14 Computer generated black dots used to show the alignment with the fixed pattern of the heating resistors. Over this 6-inch part, the glass thickness variation was within +/- 100-nm peak to peak over most of the aperture.

mountains next to deep valleys. One attempt was made to develop a piece of code that would be able to "see" the resistors and make a map of their location, but this code was never finished. In the process, we did improve the OPD flattening results on a 6-inch aperture of Borofloat as shown in figure 14.

For some tests and some edge effects, a threshold control of the heating pattern was bifurcated between 90 and 40% of the heating profile. In this way, there was continuous heating of high spots and the lower spots were allowed to cool more often. Problem, which came up once, is a place on the glass, which would not etch at all, would eventually get all the heating to no avail. This logistical challenge would abort a run. This issue may have occurred due to misalignment of the interferometer pixels to the resistor pixels. We designed a new way to resolve this discrepancy and found other related alignment problems as well.

Design of the Fresnel Lens Fizeau Interferometer;

The quality of a large diameter lenses is proportional its cost. While Fresnel, lenses used for video projection are suitable for their designed purpose they may also be used for interferometry. A point source of laser light is collimated by a Fresnel lens. This beam can be reflected from the "perfect" sheet of thin glass and returned to its origin or an adjacent point. If a camera lens can capture all of the rays returned from the glass reflection it could see an image of the fringes. While the Fresnel is not a perfect collimator, the rays are sufficiently parallel to be of use.

The required lens quality used in a Fizeau interferometer depends on the cavity length of the Fizeau interferometer and the data zeroing or flat fielding scheme. The OPD between fringes in Fizeau interferometer is 2*n*d*cos(theta). When the cavity is aligned parallel and all is perfectly collimated and mirrors flat there are no fringes. However if the collimation of the light is anything other than perfect and fringes start to appear in the parallel cavity. The Fresnel lens collimated beam has aberrations are due to fabrication on thin plastic. However, we find that the aberrations are

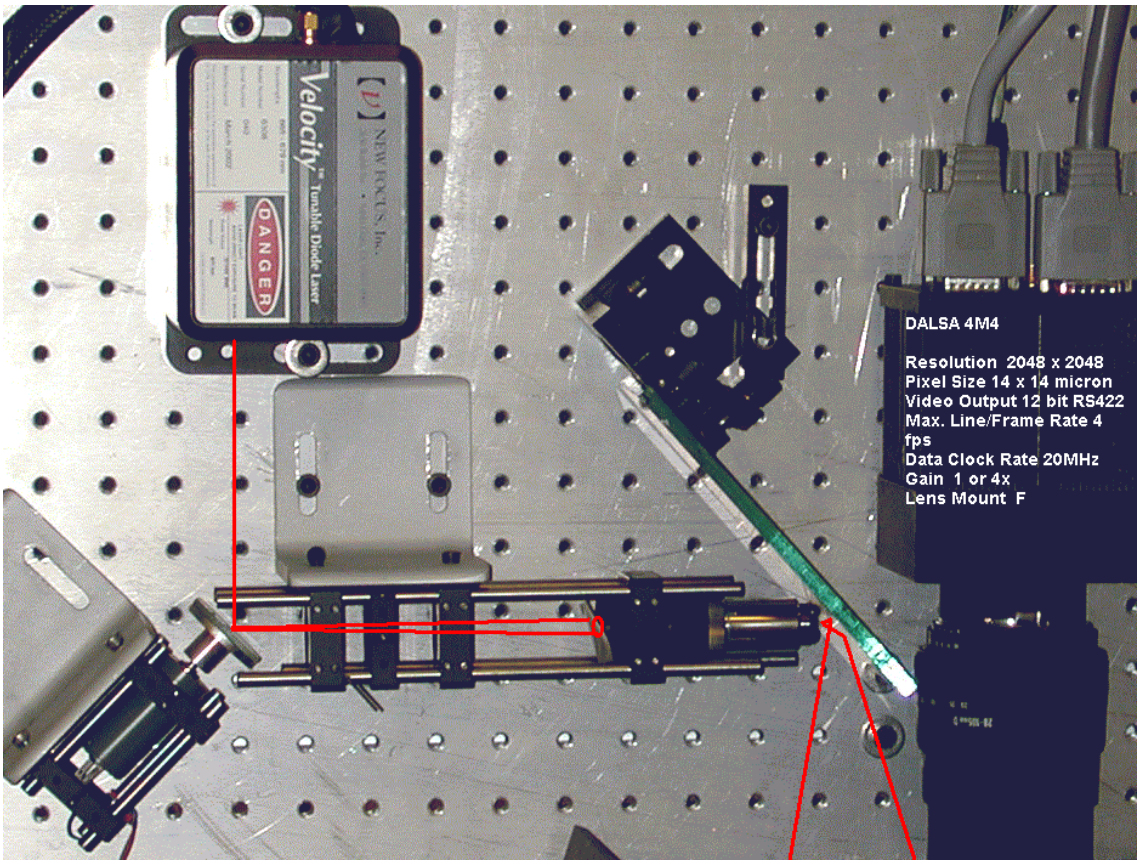

Figure 15 Tunable laser beam angularity rotated by a mirror on a motor (bottom left) reflected to an elliptical path on diffusing transparency (center). It is placed near the microscope objective so to laterally stir the speckle emanating from the microscope objective. The limiting aperture of the microscope lens sets the interferometer source size. The source and the 4m4-lens pupil are at the Fresnel lens focal distance, 1.1 Meters, and as close to one another possible to help minimize astigmatism.

small enough and do not matter as much when the Fizeau cavity thickness approaches zero. This is true for some thin (300-micron to 1 mm thick) glass, which makes up the total Fizeau cavity length. For instance, set the tolerable Fizeau fringe imperfection at 10^{th} wave. For a glass of 700 micron thickness the angle theta departure from a perfect collimator can be as large as 5x10^-3 radians or 0.3 degrees. This comes by taking the derivative of the above equation and setting the differential angle equal to the angle in error.

This implies that a lens which has a blur spot diameter of 10 mm for a 1 meter focal length would give 10^{th} wave fringe distortion when the Fizeau cavity length is 700 microns. A Fresnel lens generally is able to give about this good of a far field spot size. A better collimating lens is needed as the cavity wave front accuracy needed increases or the Fizeau cavity thickness increases, which is generally the case for most commercially available Fizeau interferometers. In either case, errors from distorted collimating lens or reference flats can be calibrated and the resulting corrupted data subtracted, as is often done at great expense in commercial systems. Our low cost system approach using the Fresnel lens is a primary result of our thin Fizeau self referencing cavity length being less than 1-mm thickness.

The F# of a good Fresnel is typically near F# 1 likewise the light source and camera lens of our interferometer are also F# 1 and only slightly off axis (Fig 15) otherwise there is Vignetting. The mirror in Fig 18, just left of center, sends the divergent light from the microscope objective down to the Fresnel lens 1.1 meters away. The light returning from the Fresnel lens then enters the camera lens, far right of this figure 15.

Fresnel lens groves create Talbot-like intensity distributions. This effect makes it hard to focus on the thin glass (where the interference fringes are located) if it is far from the Fresnel lens. In general, the thin glass is placed close as possible to the Fresnel lens and the viewing camera, which sees the Fizeau fringes, is focused onto the Fresnel lens itself. This minimizes the Talbot like interference effects. The remaining fixed pattern noise, mostly produced by the lens grove non-uniformity, is flat-fielded from the phase stepping data.

The flat-field data is gathered while inspecting a thin glass. The four phase-stepped interferogram are added together to produce a total image record of only the fixed pattern noise. This requires the Fizeau fringe phase stepping be 90 degrees. Each phase stepped interferogram is then divided by this total image to flat field away the fixed pattern noise coming from artifacts of the Fresnel lens or source non-uniformity.

The dust and lens artifacts are enhanced due to the monochromatic light used to make the interferogram. To minimize the problems in delivering a uniform intensity profile the main laser mode is stirred around on the Fresnel lens. Figure 15

The laser beam is wiggled by a mirror mounted perpendicularly with some small error to the end of a motor shaft. Light reflected from the mirror creates a circular to elliptical pattern depending on the angle of incidence. This light is directed to a translucent screen (makes small-scale speckle) just to the input side of the long conjugate side of a microscope objective. The very short FL microscope objective creates a beam spreading to nearly fill the Fresnel lens. The circularly moving mode smears laterally the speckle but the light cone appears to come from a point. This point is restricted in size due by the small diameter of the exit lens of the microscope objective. The size of the apparent circular motion must be 10 times less than the error, which would influence the position of the fringes. This depends similarly to the collimator angle requirements stated above and linearly more of a problem with increased thickness of the Fizeau cavity.

A phase stepping opportunity takes advantage of a motion of the source and camera incidence angle increases and decreases together. When doing so the fringes appear to shift. This shift follows the rules of the first stated equation. The simultaneous light source and camera movement was done by sending the illumination onto one leg of an external reflection prism while viewing the Fresnel lens reflection on the other prism leg. The prism was moved up and down relative to the interferometer optical axis and resulted in apparent angular motion of the illumination and viewing angles relative to the lens optical axis. In practice, a logistically nicer solution was to wavelength-scan as in this case it is possible to mount the illumination and camera closer together

thus reducing off axis aberrations of the Fresnel lens. Wavelength-stepping the fringes was possibility mainly a primary result of working on thin glass. Wavelength stepping for thicker Fizeau becomes a challenge to make, as the required small wavelength shifts are difficult to perform.

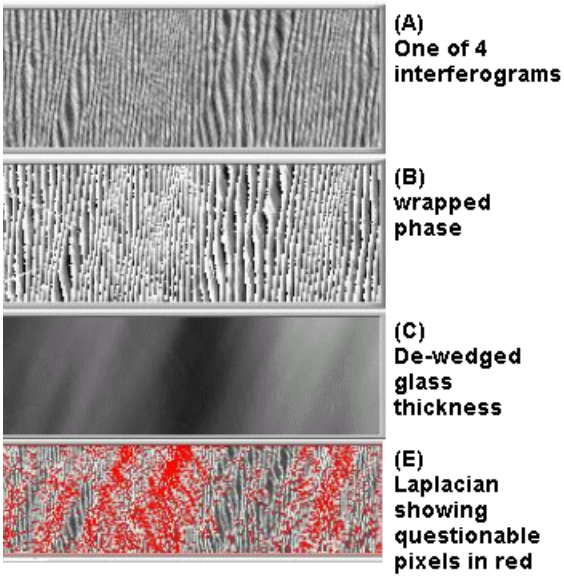

Figure 16 The fringe density for Borofloat glass samples were on the threshold of aliasing resulting in a reversal of the slope of the glass thickness measurement for the pixels marked red in (E).

Limitations in the glass wedge this interferometer can deal with.

Our approach to the fringe density being beyond the Nyquest limit of this phase unwrapping was originally dealt with by smoothing over these regions. It was felt that to locate the high and low regions would get the glass flattened enough so that these highly sloped regions of the glass would eventually produce fringe densities which would not alias. For some glass sheets it was not possible to reliably measure the small perturbations in the wedge due to the places where the fringes exceeded the Nyquest limit, see Fig 16. Therefore, we de-wedged Borofloat before making it of uniform OPD in our studies on this material.

A better collimator lens for this interferometer would extend this Nyquest limit**.**

Encircled energy plots were used to show progress in making 1737 glass of uniform OPD.

Figure 17 is a result of far field-calculation for propagation calculation to the NIF 3W focus as a piece of 1737 10 inches square was OPD flattened. Figure 10 is what the glass interference fringes looked like for each of these three cases. Further testing of these results gave similar results. The logistical problem needing to be solved is to more rapidly add and remove the acid from the glass, as

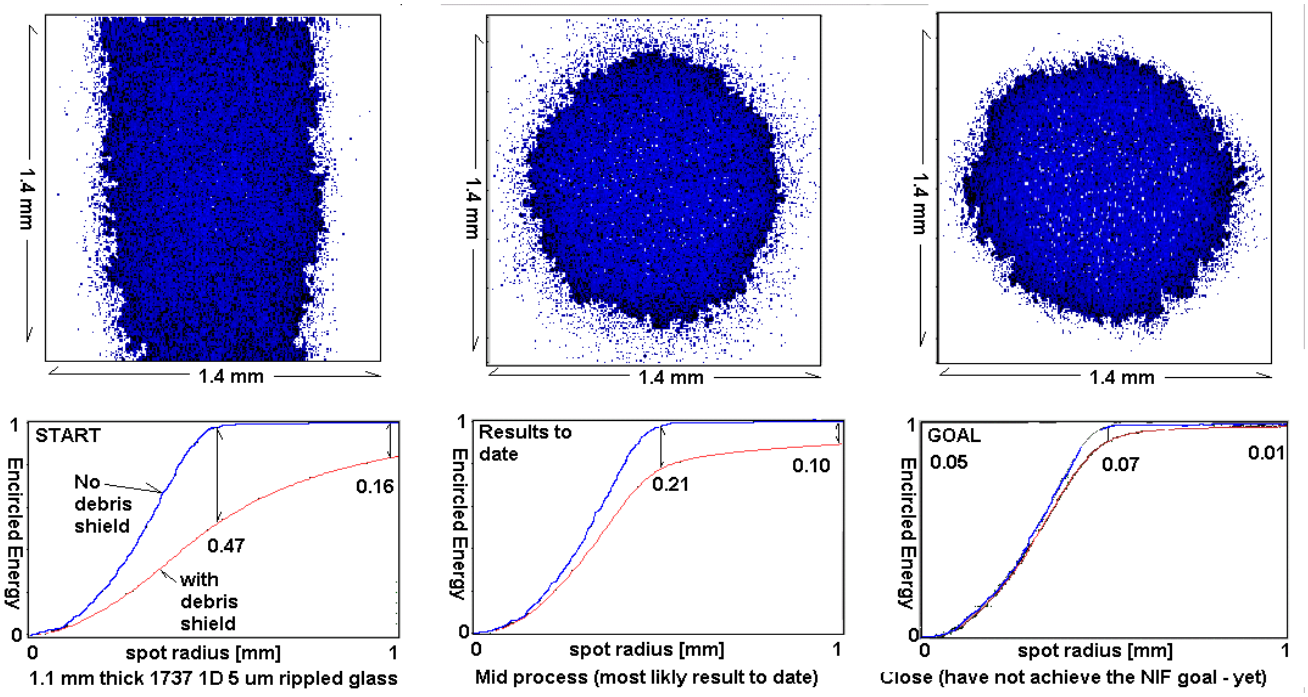

Figure 17 Encircled energy of a NIF phase plate focal spot while 1737 glass "10 inch square" is being flattened. The encircled energy goal for NIF is 5% loss maximum at 0.5 and 1 mm spot radius. These results shown a brief close approach to this need. Generally, 4X better results are needed to make the NIF standard.

this and the current interferometer code slowness limited our ability to do a full 40-cm part demo.

Wet-etch figuring offers several advantages over the conventional grind-and-polish approach

ADVANTAGES

Can polish thick or thin substrates
No stress applied to the part during polishing
No mechanical damage (e. g. scratch/dig)
No abrasive material left behind (significant for high-power laser optics)
Finish with completely closed loop controlled with real-time in-situ metrology
Process is widely tolerant to parameter variations
No calibration required
Continuous 24 hour, unattended operation possible
Tool size is flexible and can be adapted to the application
Etching of multi-component glasses has been demonstrated
Removal rates are adjustable by temperature & etchant concentration

LIMITATIONS

Optic must be chemically etchable
Optic must already possess specular surface

Conclusion;

We demonstrated it was possible to OPD flatten drawn 0.3 to 1 mm thickness glass is less than one shift. We demonstrated a 2D heater means to address figuring various regions in a parallel manner. We uncovered a way to make Achromatic AR coatings on 1737 glass. We worked around this problem and flattened glass over 10 inch square areas to sixth wave of visible light tolerances. We explored phase unwrapping codes and found some success, which need further development. We build a farm of parallel processing computer to gain a 10-fold increase in our phase unwrapping speed. We calculated the encircled energy of a NIF phase plate at NIF focus with and without the OPD imposed by the glass, we were flattening. We came to understand a need to flush the acid from the glass more often to help the rate of convergence. We found alignment problems and designed ways to accommodate, which needs further development. We made proposal on how to make modifications to all the components, which would make for a better machine. Patent disclosures Ref 4 were filed covering thermally addressed image wise wet etch figuring topic including many other approaches.

Reference:

1) "Wet-Etch Figuring: Optical Surfacing by Controlled Application of Etchant Solution Using the Marangoni Effect", M. C. Rushford, J. A. Britten, C.R. Hoaglan, I. M. Thomas, L. J. Summers, S.N. Dixit, Proc. SPIE V4451, 249-258, (2001)
URL: http://www.llnl.gov/tid/lof/documents/pdf/239898.pdf

2) Surface Contouring by Controlled Application of Processing Fluid Using Marangoni Michael C. Rushford, Jerald A. Britten U.S. Patent 6,555,017 B1 April 29, 2003
An apparatus and method for modifying the surface of an object by contracting the surface with a liquid processing solution. The liquid applicator geometry and Marangoni effect (surface-tension-gradient-driven flow) define and confine the dimensions of the wetted zone on the surface. The method and apparatus involve contouring or figuring the surface of an object using an etchant solution. The wetting fluid and real-time metrology (for example, interferometry) control the placement and dwell time of the wetted zone locally on the surface of the object, thereby removing material from the surface in a controlled manner. One demonstrated manifestation is in the deterministic optical figuring of thin glass by wet chemical etching using a buffered hydrofluoric acid solution and Marangoni effect.

3) "Wet-Etch Figuring for Precision Optical Contouring", Michael C. Rushford, Jerald A. Britten, Shamasunder N. Dixit, Curly R. Hoaglan, Michael D. Aasen, Leslie J. Summers Applied Optics, Volume 42, Issue 28, 5706-5713 October 2003

4) "Methods and systems for Optical Figuring by Image wise Heating of a solvent", Michael C. Rushford, John S. Toeppen DOE Case no. S-102,816 LLNL Docket No. IL-11216 was IL-10738 ~NOV 2001

5) "Design of a compact wide aperture Fizeau interferometer" P. R. Yoder, Jr., W. W. Hollis JOSA, Volume 47, Issue 9, 858- September 1957
"Measurement of Transparent Plates with Wavelength-Tuned Phase-Shifting Interferometry" Peter de Groot, Applied Optics, Volume 39, Issue 16, 2658-2663 June 2000

6) "Fizeau interferometer for measuring the flatness of optical surfaces" R. Bunnagel, H.-A. Oehring, K. Steiner Applied Optics, Volume 7, Issue 2, 331- February 1968

7) "Multimode laser Fizeau interferometer for measuring the surface of a thin transparent plate" Chiayu Ai Applied Optics, Volume 36, Issue 31, 8135-8138 November 1997

8) "White-light Fizeau interferometer" J. Schwider Applied Optics, Volume 36, Issue 7, 1433-1437 March 1997

9) "Influence of aberrations of Fizeau interferometer elements on measurement errors" Romuald Jozwicki Applied Optics, Volume 30, Issue 22, 3126-3126 August 1991

10) "Calibration of a 300-mm-Aperture Phase-Shifting Fizeau Interferometer" Bozenko (Bob) F. Oreb, David I. Farrant, Christopher J. Walsh, Greg Forbes, Philip S. Fairman Applied Optics, Volume 39, Issue 28, 5161-5171 October 2000

11) "Phase error calculation in a Fizeau interferometer by Fourier expansion of the intensity profile" B. V. Dorrio, J. Blanco-Garcia, C. Lopez, A.F. Doval, R. Soto, J.L. Fernandez, M. Perez-Amor Applied Optics, Volume 35, Issue 1, 61- January 1996

12) "Circuit board designed by" Jordin Kare 908 15th Ave. East Seattle, WA 98112 jtkare@attglobal.net. .

13) "LLNL Circuit Drawing" number LEA99-171611 OA
We saw a way to alter the current board so to try fewer gray levels and still deliver full power images. On the TC554001FTL memory chip, if we pull the A18 line high so to override the incoming line from the U7 chip pin 12 then we would have a 512 levels image giving us a full scale heating. Doing the same to lines A17, A16 would give us 64 levels of full scale heating. Now only have to write 64 image planes to get the thermal pattern updated and this now should take under 5 seconds to do. We did not make this change to the board since we would have to pull it from the heat sink which would likely force us to trouble shoot for shorts induced by static discharges.

14) Drawing # LEA99-171612 Rev. OA Shows the physical circuit board and component layout.

15) "Graded-index Surfaces And Films", Howard W. Lowdermilk, Ucrl-88996
URL: http://www.llnl.gov/tid/lof/documents/pdf/193325.pdf

16) "Optimal design for antireflective tapered two-dimensional subwavelength grating structures", Eric B. Grann, M. G. Moharam, Drew A. Pommet JOSA A, Volume 12, Issue 2, 333- February 1995

17) "Comparison between continuous and discrete subwavelength grating structures for antireflection surfaces", Eric B. Grann, M. G. Moharam JOSA A, Volume 13, Issue 5, 988- May 1996

18) "Two-Dimensional Phase Unwrapping : Theory, Algorithms, and Software" by Dennis C. Ghiglia (Author), Mark D. Pritt (Author) Publisher: John Wiley & Sons; (April 17, 1998) ISBN: 0471249351